BNL-209028-2018-TECH
C-A/AP/601

Overcoming proton and 3He intrinsic resonances in the AGS Booster with an ac dipole

K. Hock

September 2018

Collider Accelerator Department
Brookhaven National Laboratory

U.S. Department of Energy
USDOE Office of Science (SC), Nuclear Physics (NP) (SC-26)

DISCLAIMER

Overcoming Proton and ^{3}He Intrinsic Resonances in the AGS Booster with an ac dipole

K. Hock, F. Méot, H. Huang, N. Tsoupas, K. Zeno, J. Tuozzolo, P. Oddo
BNL C-AD, Upton, NY 11973

September 5, 2018

Abstract

Polarized ^{3}He collisions are part of future physics programs for RHIC and eRHIC. Due to optics perturbations from the AGS partial helical dipoles, it is desired to extract ^{3}He from the Booster at $G\gamma = -10.5$, which involves crossing the $12 - \nu_y$ and the $6 + \nu_y$ intrinsic resonances. To overcome these resonances, an ac dipole is being designed to be installed in the Booster. The effect of an ac dipole is to generate artificial spin-resonance by inducing vertical betatron oscillations that guide the bunch through the horizontal fields of the quadrupoles. An experimental study with Au beam was performed to confirm that the available aperture is sufficient to accommodate these large vertical betatron oscillations. Simulations for ^{3}He crossing the aforementioned resonances have been performed and display the effectiveness of the ac dipole at spin-flipping in the Booster. Due to the rapid acceleration of the Booster, the ac dipole tune will change as much as 0.0028 over the course of an ac dipole cycle, which changes the amplitude of these betatron oscillations over the course of the cycle. Through simulation, it is shown that the varying betatron amplitude does not dilute the effectiveness of the ac dipole. Sextupoles are used to provide further control over the tune spread, where RF-dual harmonics are used to control the bunch length, and to reduce the momentum spread.

Polarized protons crossing the $0 + \nu_y$ resonance has machine requirements similar to ^{3}He crossing the $12 - \nu_y$, providing a convenient proof of principle experiment for the Booster ac dipole while the ^{3}He source is being constructed; simulations of polarized protons crossing the $0 + \nu_y$ resonance have been performed as well. This paper provides an overview of the aforementioned topics and of the ac dipole functionality. Additionally, this paper lays the foundation for an ac dipole experiment, in the Booster, with protons.

Tech. Note C-A/AP/601
BNL C-AD

Contents

1 Introduction

As part of preparation for polarized ^{3}He at the RHIC accelerator complex, an ac dipole is being designed to be placed in the E3 straight section of the Booster [1, 2]. The E3 section presently houses the tune kickers and the Booster damper system. The tune kickers are in need of an upgrade since they provide usable measurements of the betatron tune at rigidities below 9.3 T $\cdot$ m, where the maximum rigidity of the Booster is 17.5 T $\cdot$ m. The damper was used to correct instabilities during high intensity proton operations [3] and thus is no longer required or operated. An ac dipole is a magnet used to induce a full spin-flip of polarized beams to prevent polarization loss through depolarizing intrinsic spin resonances. When used with ^{3}He, it will allow extraction from the Booster at a higher $B\rho$ without polarization loss. This higher injection energy into the AGS minimizes adverse effects on beam optics from the two partial helical dipoles [4] and allows injecting above the AGS $G\gamma = 0 + \nu_y$ strong resonance. To establish the ac dipole's functionality for polarized ^{3}He, it will initially be operated with polarized protons.

Unlike polarized ^{3}He that will originate from EBIS [5], polarized protons originate from C-AD's Optically Pumped Polarized Ion Source (OPPIS). They are accelerated to 200 MeV by the LINAC, and then injected into the Booster. They are typically extracted from the Booster at $G\gamma = 4.5$ to closely match the stable spin direction in the AGS [6]. This allows protons to be extracted from the Booster below the Booster $G\gamma = 0 + \nu_y$ intrinsic resonance. It is proposed that protons are extracted at $G\gamma = 4.9$, allowing the ac dipole to be used to induce a spin-flip as the $G\gamma = 0 + \nu_y$ intrinsic resonance is crossed. Requirements of the ac dipole for protons crossing the $G\gamma = 0 + \nu_y$ resonance are similar to those of polarized ^{3}He crossing the $G\gamma = 12 - \nu_y$. Additionally, the asymmetry on the AGS polarimeter is known for protons, which will be used through comparison to determine if a full spin-flip is achieved. Because of this, protons provide a convenient proof of principle.

In this Technical Note, the following aspects of the project are reviewed: An ac dipole induces a spin-flip by causing large amplitude betatron oscillations so the horizontal spin perturbing fields of quadrupoles are evenly sampled by particles in the bunch [7]. Accomodating these large oscillations requires sufficient aperture, or otherwise they incur particle losses. The documented vertical aperture was verified through a measurement with beam. This aperture was put in the zgoubi Booster model [1] to verify that it is sufficient. Previous simulations had a fixed ac dipole tune instead of a fixed frequency. It is more likely that the frequency will be fixed, which would result in the ac dipole tune to decrease as the beam is accelerated. Since the amplitude of these driven oscillations is inversely proportional to the separation between the ac dipole tune and the betatron tune, this decrease in tune will cause the oscillation amplitude to increase or decrease, depending on the tune shift of the ac dipole relative to the betatron tune. This effect does not alter the reliability of the ac dipole at spin-flipping. Because the amplitude of the coherent betatron oscillations relies on the separation between the betatron and the ac dipole tune, controlling the tune spread is very important. The benefits of having sextupoles on to control the chromaticity are addressed.

Note that, in the following, in the absence of any ambiguity, the quantity $G\gamma$, a negative value in the case of ^{3}He, may appear noted positively instead, for convenience.

2 Polarized Beams in the Booster

Polarized protons are injected into the Booster at $G\gamma = 2.18$ and accelerated to extraction at $G\gamma = 4.5$. Extraction at $G\gamma$=4.5 corresponds to when the vertical spin component, S_y, in the Booster closely matches the stable spin direction in the AGS [6, 8]. This constraint results from the two partial helical dipoles in the AGS, which because of their relative positioning in the ring, $2\pi/3$ distant azimuthally, produce a stable spin direction that is mostly vertical every [6]

$$|G\gamma| = 3n + 1.5 \tag{1}$$

(n is an integer, G=1.79285 for protons, and γ is the Lorentz relativistic factor), see Fig. 1. In the Booster, there are two types of spin resonances that are of concern: imperfection spin

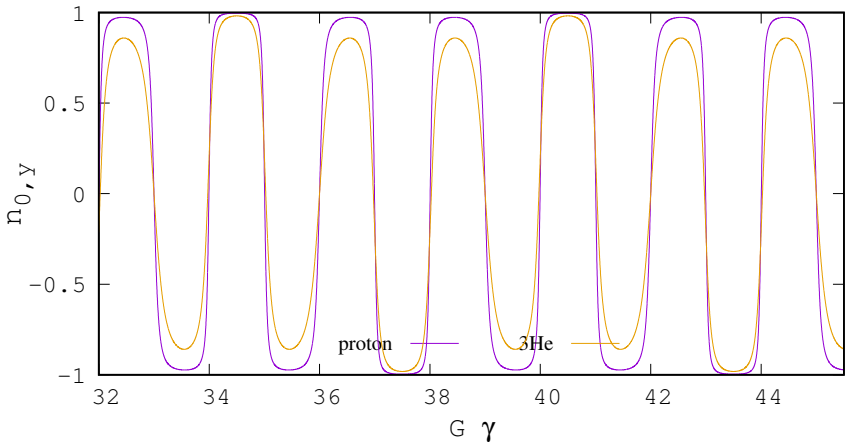

Figure 1: Modulation of the vertical $\vec{n}_0$ component, in the injection region in the AGS, in the presence of the AGS snakes, case of protons and ^{3}He with the same snake fields.

.

resonances and intrinsic spin resonances. The condition for imperfection spin resonances to occur is satisfied when [9],

$$\mathrm{G}\gamma = \mathrm{n} \tag{2}$$

as the result of a non-zero vertical closed orbit. For protons in the Booster, the $G\gamma = 3$ imperfection resonances has the orbit corrected so the beam does not experience the resonance; $G\gamma = 4$ imperfection resonances is enhanced through orbit harmonics, so the beam experiences a strong resonance and a spin-flip occurs. Vertical intrinsic spin resonances are dependent on the vertical betatron motion, occurring when [9],

$$\mathrm{G}\gamma = \mathrm{nP} \pm \nu_{\mathrm{y}} \tag{3}$$

where n is an integer, P is the periodicity (P=6 in the Booster), and ν_y is the vertical betatron tune. For protons, the only intrinsic resonance with close proximity to $G\gamma$=4.5 is at $G\gamma = 0+\nu_y$, and is avoided by keeping $\nu_y \sim 4.7$. If extraction were to occur with $G\gamma > 4.7$ or if $\nu_y < 4.5$, the 0+ resonance would be crossed. This allows ac dipole experiments in the Booster to be performed with protons, so the ac dipole would be operational when polarized ^{3}He is available in the injectors. With the partial helical dipoles in the AGS off, extraction does not need to adhere to Eq. 1 since the stable spin direction at AGS injection would be relatively well matched with Booster for all $G\gamma$ values. For the purpose of these simulations $\nu_y = 4.8088$, with extraction occurring at $G\gamma = 4.9$, so the 0+ resonance is crossed. Protons crossing the $G\gamma = 0 + \nu_y$ resonance is equally feasible with ν_y =4.1762 and extraction occurring at $G\gamma$ =4.5. Polarization of the protons will be measured in the AGS at injection. ν_y is chosen as a result of having the ac dipole frequency ,f_m, fixed at 250kHz, following

$$\text{resonant frequency } f_R = f_{rev}(m \pm \nu_s) = f_{rev}(n \pm \nu_y) \tag{4}$$

where ν_s is the spin tune.

Table 1: Table summarizing polarized species in Booster. Values for polarized ^{3}He at the $G\gamma = 12 - \nu_y$ and $G\gamma = 6 + \nu_y$ resonances are shown for reference.

	Protons				^{3}He	
	Inj.	$0 + \nu_y$	Extr. (Nominal)	Extr. (Experiment)	$12 - \nu_y$	$6 + \nu_y$
$B\rho[Tm]$	2.15	7.80	7.20	7.90	7.39	10.37
$f_{rev}[MHz]$	0.84	1.38	1.36	1.38	1.26	1.36
$E_{kin}[GeV]$	0.20	1.58	1.41	1.63	2.43	4.02
$\lvert G\gamma \rvert$	2.18	4.82	4.50	4.90	7.81	10.17

Polarized ^{3}He may encounter three intrinsic resonances, $G\gamma = 0 + \nu_y,\ 12 - \nu_y,\ 6 + \nu_y$ in a similar range of γ because of its higher anomalous magnetic moment, $G_{^3He} = -4.18415$. Due to the $\vec{n}_o$ tilt angle modulation (Fig. 1) ^{3}He should be extracted at $|G\gamma| = 7.5$ or $|G\gamma| = 10.5$. Adhering to the constraint of an ac dipole frequency of 250 kHz, the vertical tune of ^{3}He at the $G\gamma = 12 - \nu_y$ and $G\gamma = 6 + \nu_y$ resonances would be $\nu_y = 4.1891,\ 4.1744$ respectively.

2.1 Booster Model

The model of the Booster was developed in zgoubi to match a model that was developed using MADX [1, 10, 11]. A comparison of the optics for the machine configurations of protons and ^{3}He is shown in Tab. 2. As mentioned earlier, the vertical betatron tune is chosen to provide an ac dipole frequency of 250kHz. The chromaticity values shown are for sextupoles off.

2.2 Resonance Strengths

The next three sections are an overview of resonance strengths in Booster, using three different calculation methods.

Table 2: Comparison of MADX and zgoubi model results given for optics at $G\gamma = 12-\nu_y$, $G\gamma = 6+\nu_y$ for ^{3}He, and $G\gamma = 0+\nu_y$ for protons.

	Model	Orbit Length	$\nu_x,\ \nu_y$	$\xi_x,\ \xi_y$	$\beta_{max},\ \beta_{min}$
Protons 0+	MADX	201.78	4.6120, 4.8088	-7.947, -2.845	13.071, 3.906
	zgoubi	201.78002	4.6120, 4.8091	-7.378, -2.640	13.072, 3.905
^{3}He 12-	MADX	201.78	4.6150, 4.1891	-8.339, -2.195	13.916, 4.690
	zgoubi	201.78002	4.6154, 4.1888	-7.950,-1.946	13.917, 4.690
^{3}He 6+	MADX	201.78	4.6420, 4.1744	-7.699, -2.075	13.962, 4.705
	zgoubi	201.78002	4.6425, 4.1744	-6.917, -2.000	13.965, 4.705
Units		m	-	-	m

2.2.1 Froissart-Stora

Using the Froissart-Stora formula, one can calculate resonance strengths by accelerating a particle through a resonance and using the asymptotic value of the polarization after crossing the resonance, namely [12],

$$\frac{P_f}{P_i} = 2\exp(-\frac{\pi|\epsilon_k|^2}{2\alpha}) - 1 \tag{5}$$

ϵ_k is the resonance strength, P_f is the final (asymptotic) polarization, P_i is the initial polarization (far from the resonance), and α is the crossing speed, defined as [13],

$$\alpha = \frac{dG\gamma}{d\theta} = G\frac{\Delta E}{2\pi M_o} \tag{6}$$

where ΔE is the change in energy per turn and M_o is the rest mass of the particle. With a ΔE=1.68$\times 10^{-2}$ MeV/turn, the crossing speed is $\alpha = 5.105 \times 10^{-6}$ for protons. The resonance strength, ϵ_k, is the width of the resonance namely [9],

$$\epsilon_k = \frac{1}{2\pi}\oint\left[(1+G\gamma)\frac{\Delta B_x}{B\rho} + (1+G)\frac{\Delta B_s}{B\rho}\right]e^{iK\theta}\,ds \tag{7}$$

where θ is the azimuthal angle, K is the resonance condition of either Eq. 2 or Eq. 3, B_x is the radial magnetic field, B_s is the longitudinal magnetic field. This causes ϵ_k to be non-zero only when resonant conditions are met [9]. An example of a proton crossing the $G\gamma$=$0+\nu_y$ resonance is shown in Fig. 2.

2.2.2 Fresnel-Integral

Similar to the method used in the case of Froissart-Stora formula, a particle is accelerated through a weak resonance and the motion of the spin vector is tracked. The motion of the vertical spin component as it transits a weak resonance can be described with a Fresnel Integral

of the following form [14],

$$\begin{aligned} &before\ resonance\ (\theta<0): \quad (P(\theta)/P_i)^2 = 1-\tfrac{\pi}{\alpha}\epsilon_k^2\left[(0.5-C(-\theta\sqrt{\tfrac{\alpha}{\pi}}))^2+(0.5-S(-\theta\sqrt{\tfrac{\alpha}{\pi}}))^2\right] \\ &after\ resonance\ (\theta>0): \quad (P(\theta)/P_i)^2 = 1-\tfrac{\pi}{\alpha}\epsilon_k^2\left[(0.5+C(\theta\sqrt{\tfrac{\alpha}{\pi}}))^2+(0.5+S(\theta\sqrt{\tfrac{\alpha}{\pi}}))^2\right] \end{aligned} \tag{8}$$

with

$$C(x)=\int_0^x \cos(\frac{\pi}{2}t^2)dt,\ S(x)=\int_0^x \sin(\frac{\pi}{2}t^2)dt \tag{9}$$

and $\theta/2\pi$ the turn number.

This method not only provides the resonance strength but also the $G\gamma_R$ value where the resonance occurs. The Fresnel-Integral model is a weak resonance approximation, $P_f \sim P_i$. A comparison of a proton crossing the $G\gamma = 0+\nu_y$ resonance with a fit of Eq. 8 to the vertical spin component is shown in Fig. 3.

2.2.3 Static Model

A particle's spin is allowed to freely precess about the stable spin direction at a fixed $G\gamma$ value at a distance from the resonance of,

$$\Delta = G\gamma - (n\ m - \nu_y) \tag{10}$$

The average value of the vertical component of the spin at Δ can be described with,

$$\bar{S_y} = \frac{1}{\sqrt{1+|\epsilon_k|^2/\Delta^2}} \tag{11}$$

To gather usable parameters from this method, a particle is stepped through at various values of Δ surrounding the resonance, and $\bar{S_y}$ is calculated for each Δ value. A fit to the data is performed with the model as Eq. 11, in order to extract ϵ_k and the resonant $G\gamma$ value ($G\gamma_R = n\ m - \nu_y$). An example of this fit as it compares to $\bar{S_y}$ is shown in Fig. 4.

2.2.4 Comparison of Results

A summary of results from these methods can be found in Tab. 3. These results were also compared with DEPOL calculation of resonance strength from relevant MADx twiss file, all of which have excellent agreement.

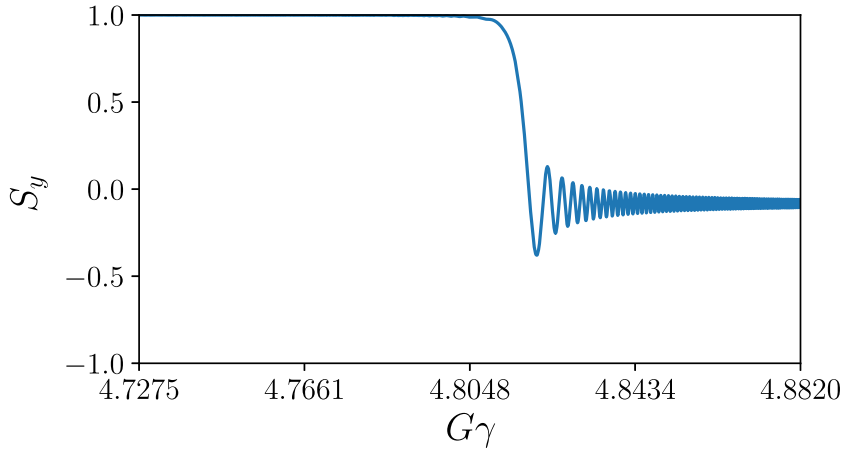

Figure 2: Froissart-Stora method. A proton crossing 0+ resonance with: vertical emittance $\varepsilon_y = 0.10\ \mu m$, $\epsilon_k = 0.001592$, $\alpha = 5.105 \times 10^{-6}$, $P_f = -8.3\%$, $\nu_y = 4.8088$

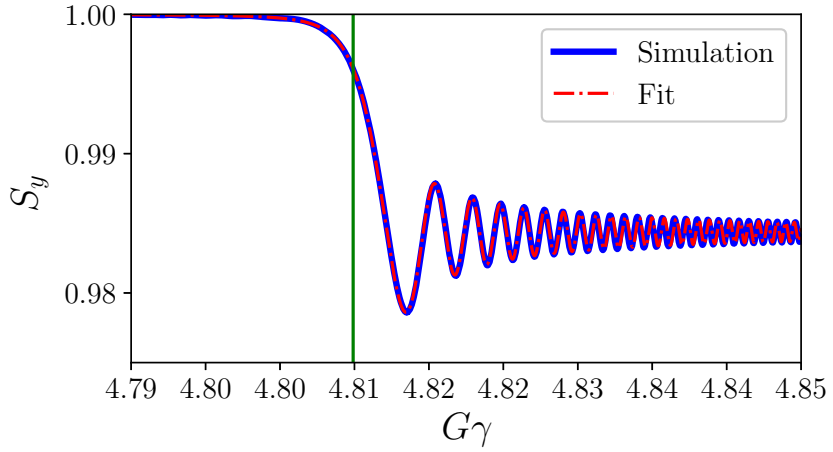

Figure 3: Fresnel integrals method. A proton crossing 0+ resonance with: vertical emittance $\varepsilon_y = 0.0001$, $\epsilon_k = 0.000160$, $\alpha = 5.105 \times 10^{-6}$, $P_f = 98.4\%$, $G\gamma_R = 4.8091$, $\nu_y = 4.8091$, and the fit model being Eq. 8.

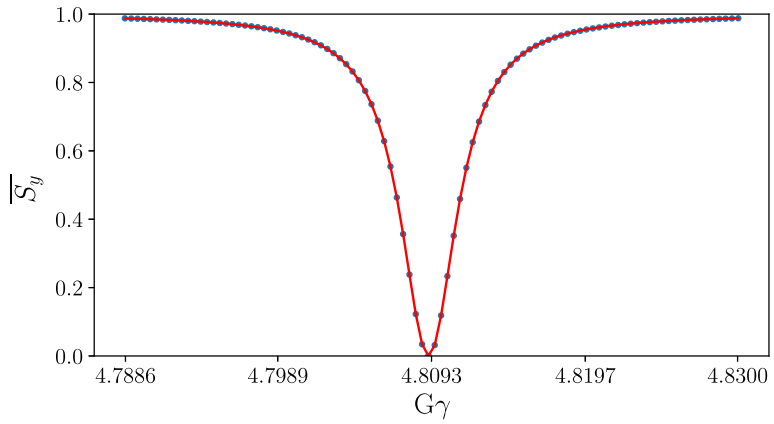

Figure 4: Fixed-$G\gamma$ spin oscillation method. Average value of the vertical spin component of a proton, for a series of $G\gamma$ values taken in the vicinity of the 0+ resonance, with: vertical emittance $\varepsilon_y = 0.234$, $\epsilon_k = 0.002463$, $G\gamma_R = 4.8091$, $\nu_y = 4.8091$

Table 3: Summary of resonance strengths calculated with various methods. $\alpha_{protons} = 5.105 \times 10^{-6}$; ^{3}He crossing 12- resonance uses a fast ramp rate of $\alpha_{^3He,12-} = 7.961 \times 10^{-6}$ where the 6+ resonance crossing uses a slow ramp rate of $\alpha_{^3He,6+} = 2.6537 \times 10^{-6}$. These results are compared with results from DEPOL, which calculates the resonance strength from a MADx Twiss file [15].

	Resonance	Froissart-Stora		Fresnel Integral		Static		DEPOL
$\varepsilon_y(\mu m)$		ϵ_k	P_f	ϵ_k	ν_y	ϵ_k	ν_y	ϵ_{0+}
Protons								
0.001	$0+\nu_y$	0.000160	0.984	0.000160	4.8091	0.000161	4.8091	0.000161
0.1		0.001592	-0.083			0.001606	4.8091	0.001614
0.234						0.002463	4.8091	0.002469
10						0.016205	4.8094	0.016137
^{3}He								
0.001	$12-\nu_y$	0.000135	0.993	0.000135	7.8079	0.000132	7.8082	0.000130
0.1		0.001350	0.396			0.001319	7.8082	0.001303
0.535						0.003037	7.8082	0.003013
10						0.013319	7.8082	0.013027
0.001	$6+\nu_y$	0.000229	0.933	0.000238	10.1739	0.000226	10.1742	0.000224
0.1		0.002291	-0.916			0.002265	10.1742	0.002235
0.369						0.004396	10.1742	0.004294
10						0.022826	10.1742	0.022353

2.3 Vertical Aperture near ac dipole

A study was performed with Au during RHIC Run of 2017 (Run17) to confirm documented vertical aperture. A vertical bump was made 25 ms into the cycle at the B7 location in both directions, +13.5 mm and −12.5 mm, where a small loss was generated (the measurement had to be done close to injection due to correctors that are too weak to make a bump large enough to generate a loss at higher $B\rho$). Emittance from the Booster is measured with multiwires in its extraction line; the most commonly used is the first multiwire, six feet into the extraction line, called MW006. An emittance measurement from MW006 was $\varepsilon_{\mathrm{y,N,rms}} = 3.7\ \pi$ mm mrad, where $\varepsilon_{\mathrm{y,N,rms}}$ is the normalized RMS emittance. This value was extrapolated back to the unnormalized emittance where the aperture measurement was done, $\varepsilon_{\mathrm{y,rms,25\ ms}} = 49.3\ \pi$ mm mrad. The limiting aperture in the vertical plane is from the dipole vacuum pipe, ±35 mm. Through this study, the vertical aperture was verified to be 35 mm from center, as shown in Fig. 5.

A ferrite magnet is being designed for use as an ac dipole, which will be installed in vacuum at E3. The following analysis is performed to ensure the magnet will not become the limiting aperture of the machine. The magnet is going to be 50 cm long, and be placed approximately 20 cm after vacuum equipment that proceeds the QVE3 quadrupole. The aperture of this magnet is going to be 8.6 cm horizontally and 8.2 cm vertically (because of the 2mm copper conductor on the top and bottom of the magnet). The

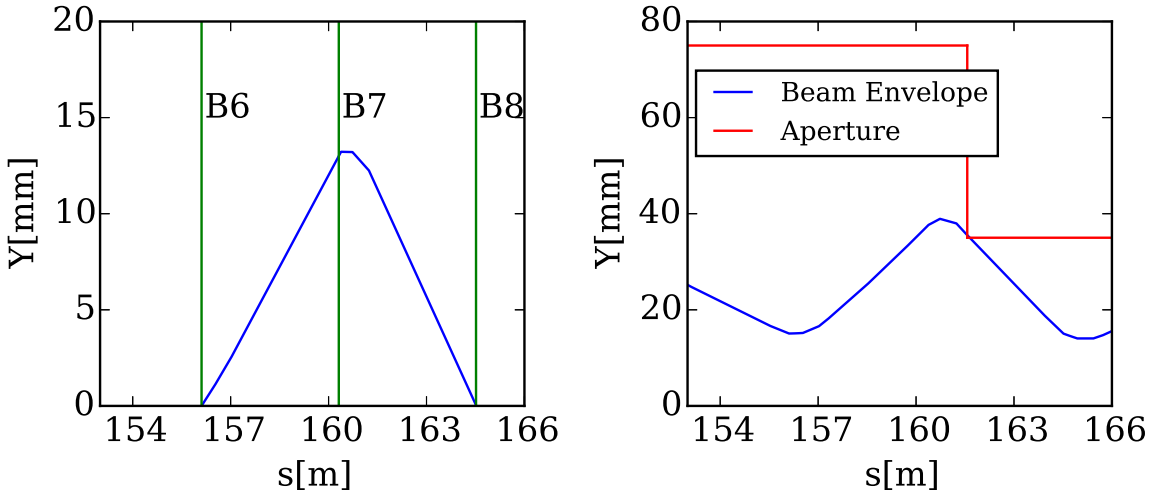

Figure 5: Left: Vertical orbit used to generate the small loss at B7. Right: Full-width of beam envelope with the addition of the orbit bump (left) in blue, with the addition of known aperture in red [16, 17].

maximum horizontal and vertical beam envelopes at the magnets' position provide the minimum aperture limits of 64.252 mm and 64.094 mm, excluding any alignment errors. Recent survey data [18] shows a maximum alignment error of 3 mm vertically and 10 mm horizontally as seen in Fig. 6. Accounting for the beam envelope and alignment errors, the magnet aperture provides a buffer of approximately 14.9 mm vertically (82.0 mm - 64.1 mm - 3 mm) and 11.7 mm horizontally (86.0 mm - 64.3 mm - 10 mm) before becoming the limiting aperture of the machine. The horizontal and vertical beam envelopes, as well as the aperture corresponding to magnet placement, are shown in Fig. 7.

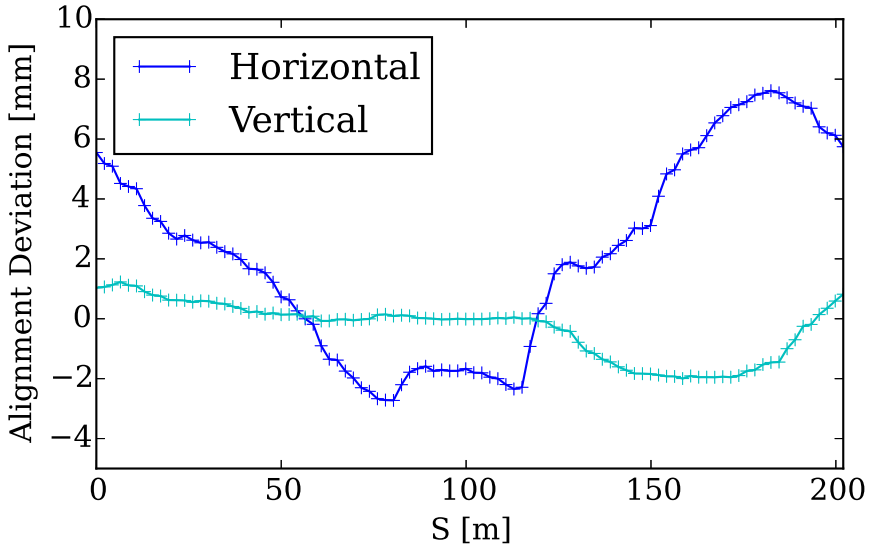

Figure 6: Vertical and Horizontal alignment deviations from zero from most recent survey data [18]. The maximum and minimum excursions are +7.62 mm and -2.73 mm horizontally (10.34 mm difference) and 1.23 mm and -2.00 mm vertically (3.22 mm difference).

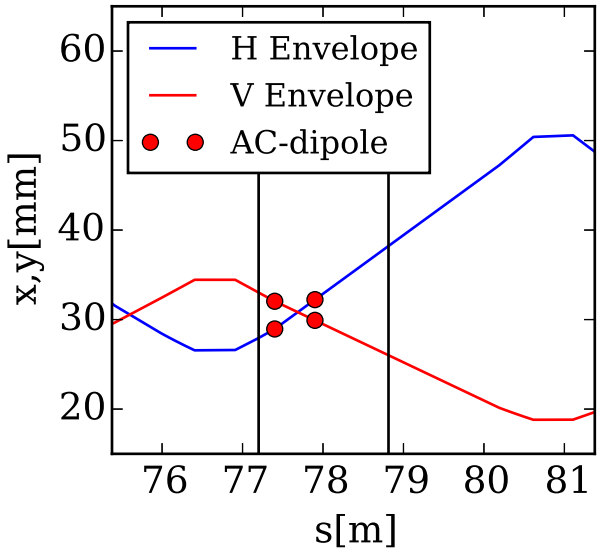

Figure 7: Beam envelope for horizontal (blue) and vertical (red) for the E3 section. The area between E3 vacuum equipment assembly and the WCM are the two black lines, the beam envelope value that coincides with the placement of the magnet are red circles with horizontal and vertical beam envelope (minimum and maximum) values of (28.949 mm, 32.226 mm) and (32.047 mm, 29.914 mm) respectively.

3 ac dipole

An ac dipole is a magnet that enhances the strength of intrinsic resonance, by forcing the entire bunch to undergo large betatron oscillations [19]. It drives these oscillations with a sinusoidally oscillating field in phase with the betatron motion. These large oscillations cause all particles to sample the depolarizing horizontal fields experienced in quadrupoles. The amplitude of these driven oscillations is defined as,

$$Y_{coh} = \frac{B_m l}{4\pi B\rho \delta_m}\beta_{yk} = \frac{\beta_{yk}\theta_k}{4\pi\delta_m} \tag{12}$$

where β_{yk} is the amplitude of the beta function at the location of the ac dipole; $\theta_k = B_m l/B\rho$ is the deflection angle from the magnet with field B_m, and length l, at rigidity $B\rho$; the resonance proximity parameter, δ_m, is,

$$\delta_m = \nu_y - (k - \nu_m). \tag{13}$$

where ν_m is the modulation tune of the ac dipole, defined as,

$$\nu_{\mathrm{m}} = \mathrm{f_m}/\mathrm{f_{rev}}. \tag{14}$$

The Froissart-Store formula can be extended to a Gaussian beam distribution with a large betatron amplitude, so the expectation value of the ratio of asymptotic polarization values with an ac dipole can be calculated. This has the form [9],

$$\left\langle \frac{P_f}{P_i} \right\rangle = \frac{2}{1+\frac{\pi|\epsilon_k|^2}{\alpha}} \exp\left\{ -\frac{(\frac{(\beta_{yk}\theta_k)^2}{2\sigma_y^2})\frac{\pi|\epsilon_k|^2}{\alpha}}{1+\frac{\pi|\epsilon_k|^2}{\alpha}} \right\} - 1 \tag{15}$$

where σ_y is the RMS beam width at the ac dipole location. Eq. 15 can be rearranged in order to get the bunched beam requirement for a 99% spin flip, which is approximately

$$\beta_{yk}\theta_k \geq \left[-2 \ \ln\left(0.005\left(1+\frac{\pi|\epsilon_k|^2}{\alpha}\right)\right)\left(1+\frac{\alpha}{\pi|\epsilon_k|^2}\right)\right]^{1/2}\sigma_y. \tag{16}$$

Because $\nu_m \neq \nu_y$ it also creates a second resonance at a distance of δ_m away from the intrinsic resonance. To determine ac dipole strength, simulations are required for the two resonances with such a close proximity.

A caveat of having an ac dipole in the Booster is the rapid change in revolution frequency. This rapid change will cause a change in δ_m while the ac dipole is exciting the beam, causing the amplitude from Eq. 12 to either increase (in the case where $\delta_m > 0$, causing ν_m to drift closer to ν_y) or decrease (in the case where $\delta_m < 0$, causing ν_m to drift away from ν_y) during the cycle, rather than remain constant. This is shown in Fig. 8 where ν_m decreases as a result of increasing f_{rev}. To ensure the constrained ac dipole frequency is recovered, the frequency is calculated with variables from simulations, $\nu_{m,o} = 0.1912$ and $f_{rev,o} = 1.3796$ MHz, which yields the constrained value of $f_m = 250$ kHz.

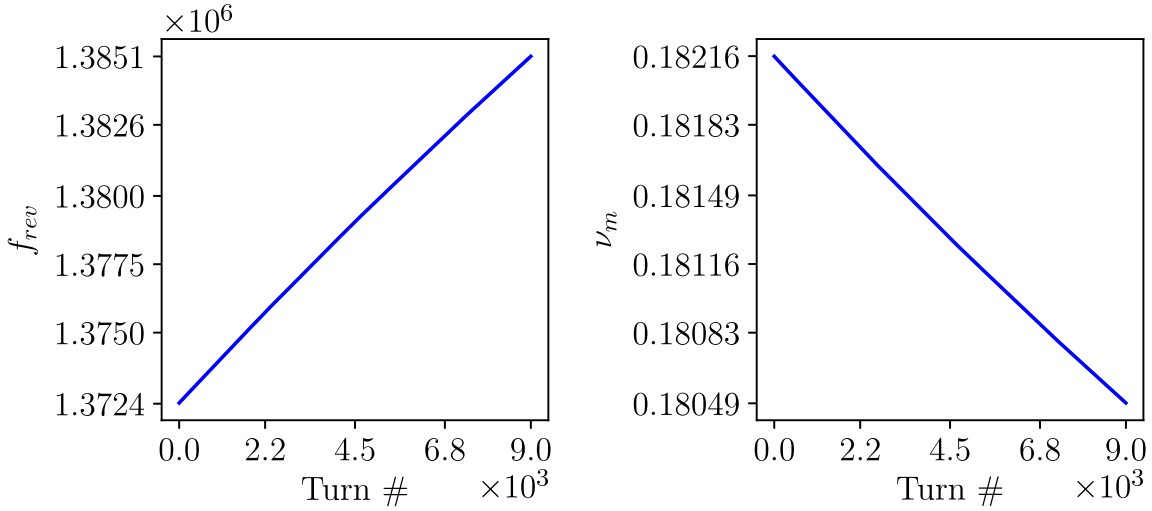

Figure 8: Figure above shows the change in f_{rev} (left) as the beam is accelerated and the resulting change in ν_m (right) when f_m=250 kHz.

3.1 Chromaticity

To ensure that the beam is not scraped on the aperture while undergoing these large betatron oscillations, it is important to keep the tune spread minimal. The deviation of vertical tune with respect to a change in momentum is defined as [20],

$$\delta_{\nu_y} = \xi_y \delta_p \tag{17}$$

where ξ_y is the vertical chromaticity, and $\delta_p = (p - p_{ref})/p_{ref}$ is the relative momentum deviation of the particle. During RHIC run 17, the full-width at half-maximum of the momentum spread for protons was 1.39×10^{-3}, resulting in $\sigma_{\mathrm{p}} = 1.18 \times 10^{-3}$ if a normal distribution is used. The resulting coherent amplitude (Eq. 12) resulting from the full-width of the momentum spread is shown in Fig. 9 for the natural vertical chromaticity, $\xi_{y,nat}$=-2.64, and for ξ_y=-0.5. The very large coherent amplitude observed in Fig. 9 for $\xi_{y,nat}$ will cause beam loss since the particles would be outside the physical aperture, where the coherent amplitude with ξ_y=-0.5 is safely inside the aperture. The maximum vertical amplitude particle from tracking particles through the $G\gamma = 0 + \nu_y$ resonance with various chromaticity values and the ac dipole on is shown in Tab. 4.

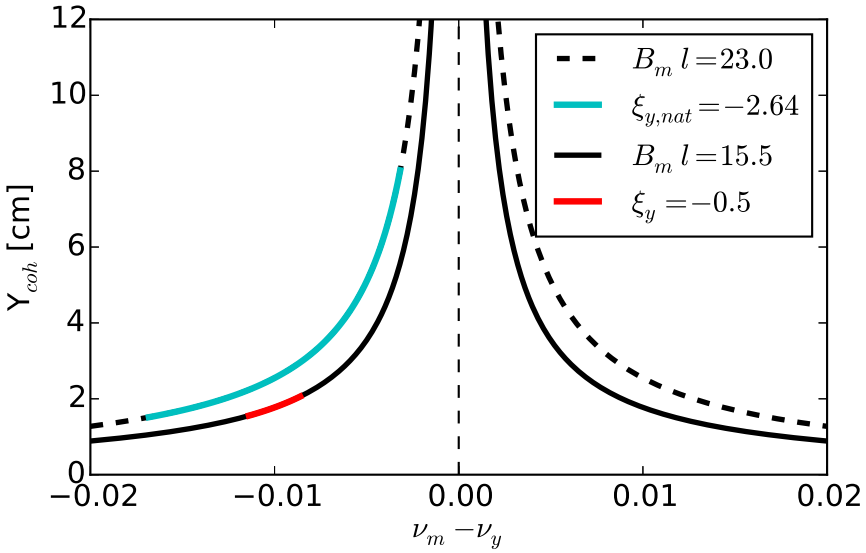

Figure 9: Comparison of expected vertical coherent amplitudes with an ac dipole for full-width of momentum spread. The natural chromaticity of the machine (red) and ξ=-0.5 (cyan).

Table 4: Table summarizing the effects of various vertical chromaticity settings. Note that lower chromaticities correspond to lower field requirements and a lower maximum vertical amplitude of the beam.

ξ_y	-0.5	-1.0	-1.5	-2.64
$B_m \cdot l$ [G · m]	16.0	18.0	19.6	23.0
$Y_{coh,max}$ [cm]	2.38	2.99	3.58	7.91

3.2 RF Dual-Harmonic

There are several benefits of utilizing dual RF harmonics operationally in the Booster. The primary function is to minimize space charge effects by making a uniform longitudinal charge distribution, so to reduce emittance growth [21]. An additional benefit is to reduce the momentum spread, which reduces the tune spread. It is for the second reason why dual harmonics are utilized with the ac dipole on. The equation of motion for a particle in a double RF system is defined as [9],

$$\dot{\delta} = \frac{\omega_{rev} e V_1}{2\pi\beta^2 E}\left[\sin\phi - \sin\phi_{1s} + \frac{V_2}{V_1}\left[\sin\left(\phi_{2s} + \frac{h_2}{h_1}(\phi - \phi_{1s})\right) - \sin\phi_{2s}\right]\right] \tag{18}$$

where ω_{rev} is the revolution frequency, e is the charge, β is the velocity, E is the energy, V is the voltage of the cavity, ϕ_s is the synchronous phase, h is the harmonic number, indices 1 and 2 for respectively the first and the second cavity. The RF parameters used for this double RF system are $V_1 = 32$ kV, $V_2 = 10$ kV, $\phi_{1s} = \pi/6$, $\phi_{2s} = \pi$, h_1=1, h_2=2. This produces a longitudinal density that is flattened. A comparison of the RF Bucket for the single-harmonic and dual-harmonic configurations is show in Fig. 10. By comparison of the bucket height, it is determined that the maximum momentum deviation is reduced by 20%.

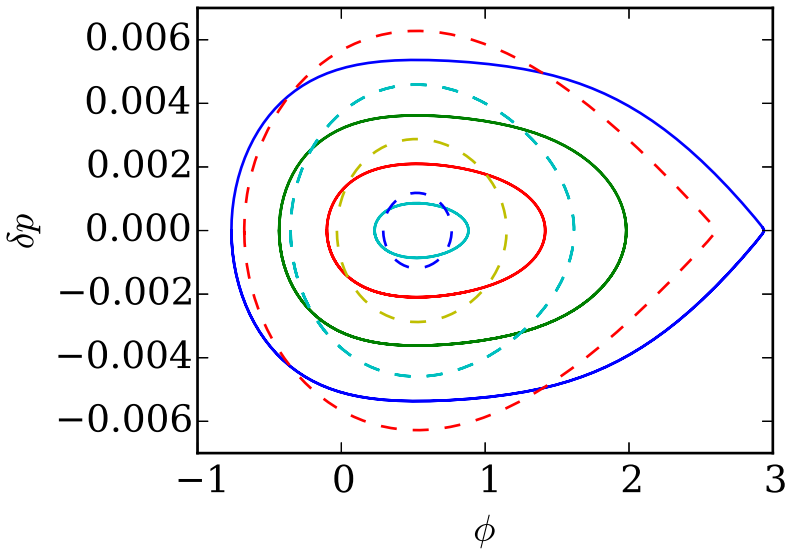

Figure 10: Comparison of the single harmonic bucket (dashed lines) and the elongated dual harmonic bucket (solid lines).

For the comparison of a single harmonic with a dual harmonic, it is common to compare ratio of peak current to bunch length, where bunch length refers to the full-width of the longitudinal distribution. From measurements taken on a scope, this ratio for the dual harmonic bucket is 0.38, and for the single harmonic is 0.69. The comparison of these two ratios shows the peak current to bunch length for dual harmonics is 55% of the single harmonic. To ensure that the double harmonic is appropriately setup in zgoubi, 1,000 particles are tracked for several synchrotron periods, T_s, and a histogram is taken of the longitudinal distribution. Fig. 11 shows the longitudinal distribution of 1,000 particles for the single and double harmonic case. The comparison of height to length ratio for these two distributions gives a dual harmonic ratio that is 56% of the single harmonic bucket. Additionally, the maximum amplitude in the vertical plane was also reduced by 12%, and the field required to get a full spin flip was reduced by 13%, as noted in Tab. 5.

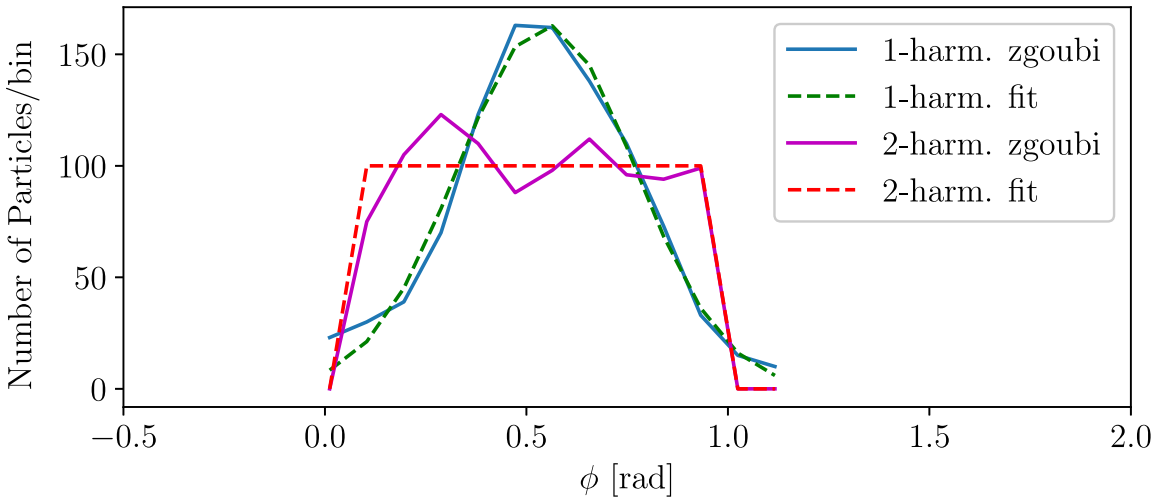

Figure 11: Comparison of longitudinal distributions between a single harmonic RF cavity setup and a dual harmonic RF cavity.

Table 5: Comparison of ac dipole requirements and maximum coherent amplitude of the beam for the single and dual harmonic case.

	1 Harmonic	2 Harmonic
$B_m l$ [G m]	15.50	13.85
$Y_{coh,max}$ [cm]	2.39	2.05

3.3 Spin Tracking Results

For these simulations, a vertical normalized 95% emittance of $\varepsilon_{\mathrm{y,N95\%}} = 3.5\ \pi$ mm mrad is used, which is the largest emittance value observed on MW006, during initial stages of proton setup for Run17. The value of Gγ at the start of simulations, Gγ_{o}, is determined using:

$$\mathrm{G}\gamma_{\mathrm{o}} = \mathrm{G}\gamma_{\mathrm{R}} - \pi\alpha\ \mathrm{N} \tag{19}$$

where $G\gamma_R$ is the resonant $G\gamma$ value that particles are being tracked through, and N is the total number of turns for the ac dipole ramp.

3.3.1 Variable ν_m

Ideally, ac dipole driving tune should be fixed, but the driving frequency is fixed in reality. Ac dipole simulations were done with a fixed modulation frequency, and a fixed modulation tune [1], for comparison. The change in tune over the course of the ramp, $\Delta\nu_m$, was calculated for the fixed frequency simulations. The start of the ramp was chosen so that,

$$\nu_{m,0} = \nu_m + \Delta\nu_m/2 \tag{20}$$

and would end with,

$$\nu_{m,N} = \nu_m - \Delta\nu_m/2 \tag{21}$$

For protons, the change in ac dipole tune is $\Delta\nu_m = 0.0017$ which involved an 8,000 turn ac dipole cycle. For helions crossing the $G\gamma = 12 - \nu_y$, $\Delta\nu_m = 0.0028$ for a 5,600 turn ac dipole cycle; crossing the $G\gamma = 6 + \nu_y$, $\Delta\nu_m = 0.00089$ for 17,000 turns. For these cycles $\delta_m = 0.01$, so the amplitude of the oscillations increases during the cycle as a result of decreasing ν_m. This effect does not change the ac dipole strength required to achieve a 99% spin-flip, but provides a more constant coherent amplitude.

Fig. 12 shows the Fast Fourier Transform (FFT) spectrum of the vertical particle motion for fixed ν_m and fixed f_m. A peak corresponding to the coherent motion from the ac dipole is evident, as well as the peak associated with the betatron motion. The ac dipole peak associated with the fixed f_m shows a clear broadening as a result of the sweep ν_m goes through.

3.3.2 Comparison with Theoretical Requirement

To obtain a result that compares closely with the theoretical requirement of the ac dipole (in Eq. 16), δ_m (in Eq. 13) was reduced so the two resonances overlap. The requirement found from these simulations are in Tab. 6.

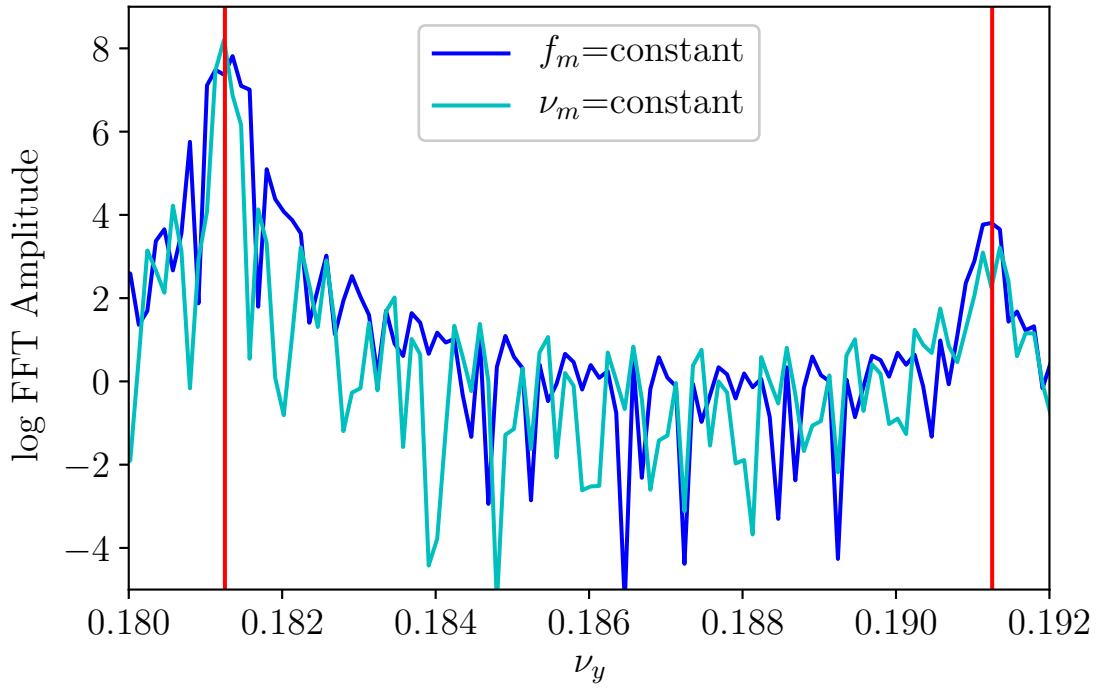

Figure 12: Two FFT spectra are shown corresponding to ν_m=constant (cyan) and f_m=250 kHz (blue). The betatron peak and the ac dipole peak are marked with red vertical lines, and have a separation of δ_m=0.01.

Table 6: $B_m \cdot l$ shows good agreement with theory (values in parenthesis) when δ_m is brought close to zero so the two resonances are sufficiently overlapped. β_{max} = 13.6 m, $\beta_k \sim$ 11 m, ε_{ratio} is the ratio of final and initial normalized emittances to quantify growth. $N_{scraped}$ is the percentage of particles lost on the aperture.

	Protons	^{3}He	
Resonance	$0+\nu_y$	$12-\nu_y$	$6+\nu_y$
ϵ_k	0.00246	0.00304	0.00440
σ_y [mm]	1.83	2.75	2.31
$B_m \cdot l$ [G m], $\delta_P = 0$	4.84 (4.34)	6.5 (5.91)	6.0 (5.89)
$B_m \cdot l$ [G m]	15.5	16.5	20.5
f_m [kHz]	250	250	250
ε_{ratio}	1.03	1.02	1.00
$N_{scraped}/N_{total}$[%]	0.0	1.2	0.0

4 Run 19 Proton Experiment

The ac dipole will be installed in the Booster in 2018. An experiment is planned for Run19 with protons crossing the $G\gamma = 0 + \nu_y$ resonance. Results from simulations of protons crossing the $G\gamma = 0 + \nu_y$ can be seen and Fig. 13. This will involve extracting from the Booster at $G\gamma = 4.9$ with ν_y=4.809, so the $G\gamma = 0 + \nu_y$ resonance can be crossed. As mentioned earlier, ν_y=4.809 is a constraint on the tunes resulting from a

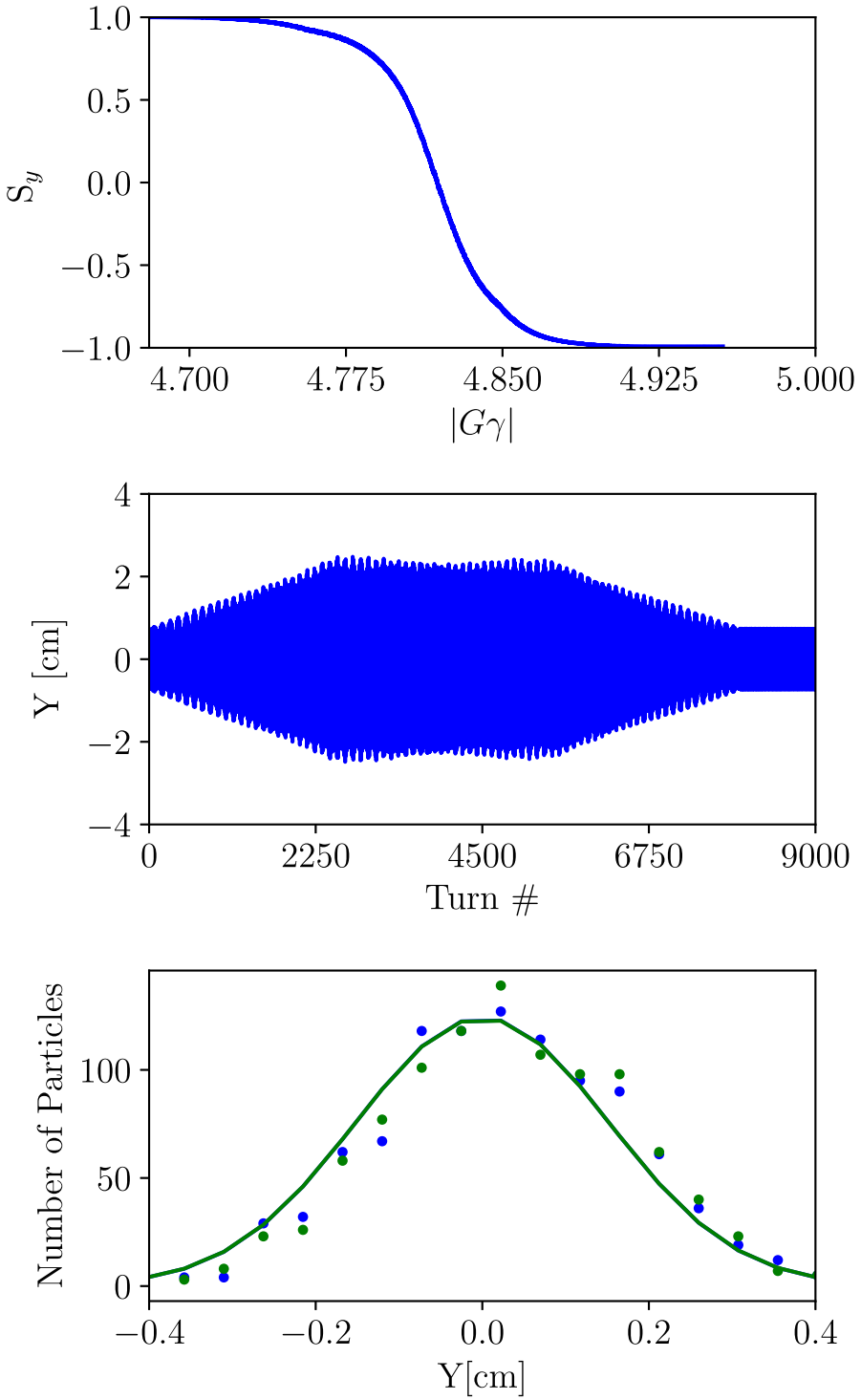

Figure 13: $G\gamma = 0+$, $\nu_y = 4.8089$, $\nu_m = 1 - (Q_y + 0.010)$, $\Delta B_m l = 15.5$ G · m, $P_f = -99.0\%$, $\varepsilon_r = 1.03$. (top) The vertical component of the spin vector as the resonance is crossed with the ac dipole on. (center) Amplitude of the vertical bunch motion during the ac dipole ramp. (bottom) Final bunch distribution (green) and initial distribution (blue) used to calculate the change in normalized emittance.

250 kHz ac dipole frequency. Due to the lack of polarimetry in the Booster, polarization will be measured in AGS at injection. This will require the AGS partial snakes to be off, so the condition of Eq. 1 does not need to be met, and the stable spin direction between the Booster and AGS are well matched.

5 Conclusion

The simulations show that the ac dipole can overcome the intrinsic resonance at $G\gamma = 0 + \nu_y$ in Booster. We have confirmed the size of the aperture and determined that there is sufficient aperture available to achieve a full spin flip with negligible beam loss. The criteria for a full spin-flip of protons crossing the $G\gamma = 0 + \nu_y$ is similar to that of ^{3}He at $G\gamma = 12 - \nu_y$, providing a convenient proof of principle experiment. These simulations were done with a fixed modulation frequency of the ac dipole which mimics the operating mode that is more realistic. It was determined that the resulting modulation tune sweep does not dilute the effectiveness of spin-flipping. With sextupoles turned on, the maximum amplitude of the coherent oscillations was reduced as a result of controlling the tune spread.

Appendix

^{3}He Spin Tracking Results

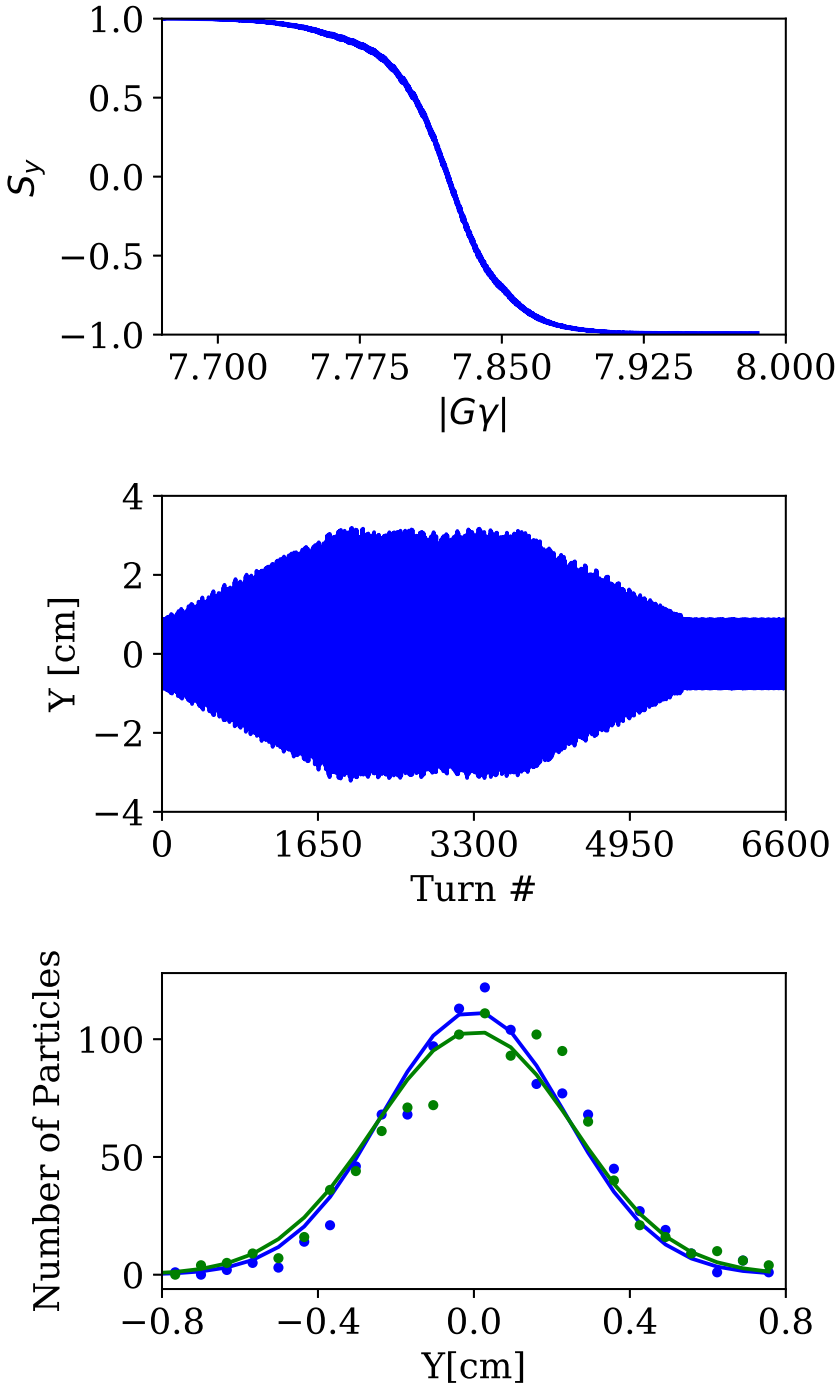

Figure 14: $G\gamma = 12-$, $\nu_y = 4.189$, $\nu_m = \nu_y + 0.010$, $\Delta B_m l = 16.5$ G · m, $P_f = -99.0\%$, $\varepsilon_r = 1.04$. (top) The vertical component of the spin vector as the resonance is crossed with the ac dipole on. (center) Amplitude of the vertical bunch motion during the ac dipole ramp. (bottom) Final bunch distribution (green) and initial distribution (blue) used to calculate the change in normalized emittance.

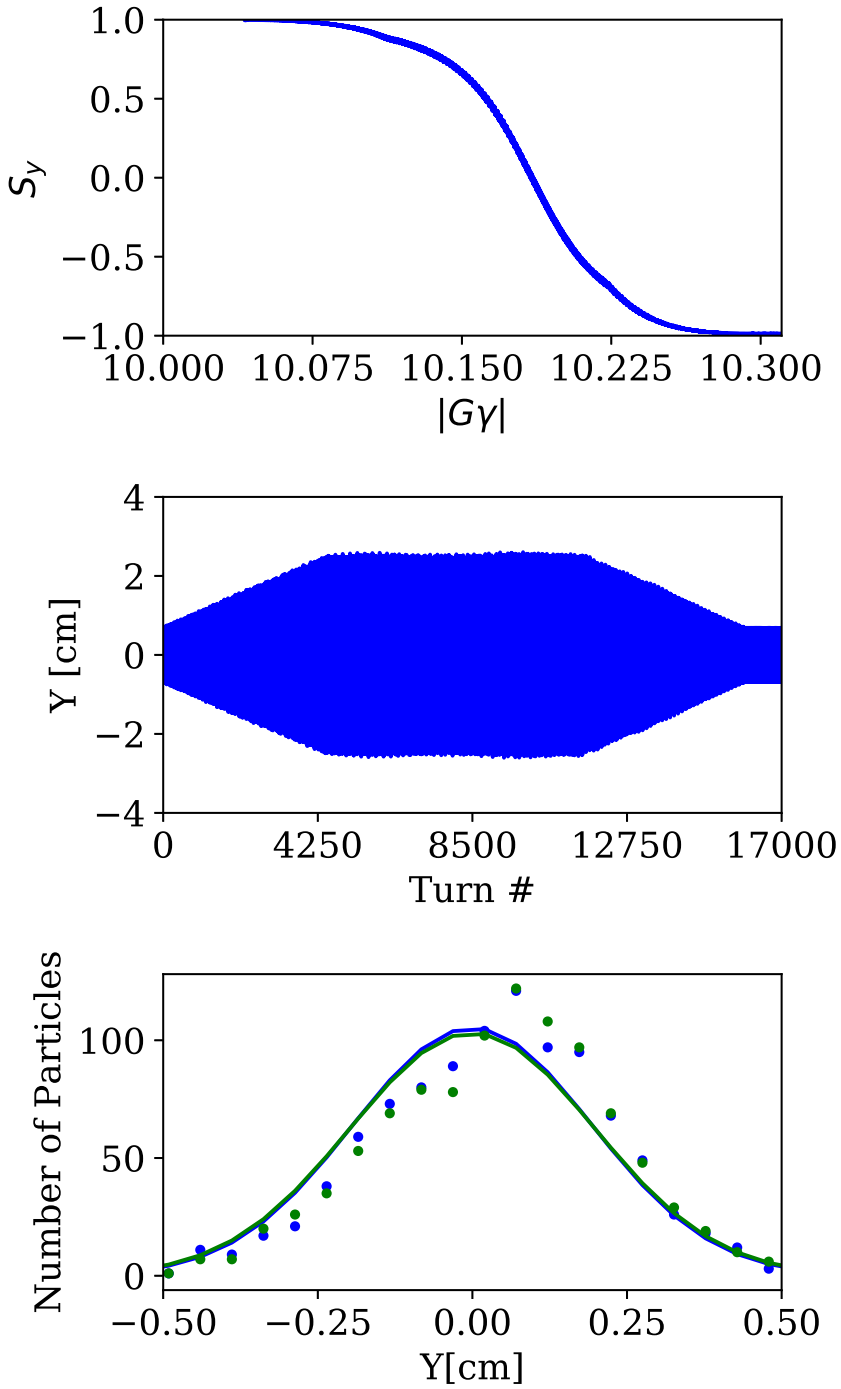

Figure 15: $G\gamma = 6+$, $\nu_y = 4.174$, $\nu_m = \nu_y + 0.010$, $\Delta \mathrm{B_m l} = 21.0$ G·m, $P_f = -99.0\%$, $\varepsilon_r = 1.06$. (top) The vertical component of the spin vector as the resonance is crossed with the ac dipole on. (center) Amplitude of the vertical bunch motion during the ac dipole ramp. (bottom) Final bunch distribution (green) and initial distribution (blue) used to calculate the change in normalized emittance.

References

[1] K. Hock et al., *Intrinsic Resonances and AC-Dipole simulations of ^{3}He in the AGS-Booster*, C-AD Tech Note 597 (2017).

[2] N. Tsoupas et al., "An AC-Dipole for the AGS Booster to overcome spin resonances for polarized $^3He^{2+}$," in *Proceedings CAARI 2018 Conference.* Dallas, USA (2018).

[3] D. Russo et al, "Results From the AGS Booster Transverse Damper," in *Proceedings of Particle Accelerator Conference 1993.* Washington D.C., USA (1993).

[4] A. Luccio et al., *Cold AGS Snake Optimization by Modeling*, C-AD Tech Note 128 (2003).

[5] J. Maxwell et al, "Development of a Polarized He-3 Source for RHIC and eRHIC," in *Proceedings of Spin2014.* Beijing, China (2014).

[6] F. Lin, *Towards Full Preservation of Polarization of Proton Beams in AGS*, Ph.D. thesis, Indiana University (2007).

[7] M. Bai, *Overcoming the Intrinsic Spin Resonance by Using an RF Dipole*, Ph.D. thesis, Indiana University (1999).

[8] H. Huang et al, "Overcoming Depolarizing Resonances in the AGS with Two Helical Partial Siberian Snakes," in *Proceedings of Particle Accelerator Conference 2007.* Albuquerque, USA (2007).

[9] S. Y. Lee, *Spin Dynamics and Snakes in Synchrotrons* (World Scientific Publishing Company Incorporated, 1997).

[10] K. Brown et al., *A high precision model of Booster Tune Control*, C-AD Tech Note 69 (2002).

[11] F. Méot, *Zgoubi User's Guide*, https://sourceforge.net/projects/zgoubi/.

[12] M. Froissart, R. Stora, "Depolarisation d'un faisceau de protons polarises dans un synchrotron," Nuclear Instruments and Methods **7:297-305** (1959).

[13] F. Méot, *Spin Tracking simulations in AGS based on ray-tracing methods - bare lattice, no snakes*, C-AD Tech Note 452 (2009).

[14] G. Leleux, "Traversée des résonances de dépolarisation," (1991), unpublished.

[15] V. Ranjbar et al., "Mapping out the full spin resonance structure of RHIC," in *Proceedings of Particle Accelerator Conference 2001.* Chicago, USA (2001).

[16] A. Luccio, *Booster Chamber Aperture*, Booster Tech Note 202 (1991).

[17] S. Y. Zhang, *Booster Horizontal and Vertical Aperture*, AGS Studies Report No. 360 (1997).

[18] C. Yu et al., "AGS Booster Adjustment Report," (2015), unpublished.

[19] H. Huang et al., *Overcoming the Intrinsic Spin Resonance using Resonance Island created by RF Dipole*, C-AD Spin Note 055 (1997).

[20] S. Y. Lee, *Accelerator Physics* (World Scientific Publishing Company Incorporated, 2012).

[21] H. Huang et al., "AGS Polarized Proton Operation Experience in RHIC Run17," in *Proceedings of International Particle Accelerator Conference 17* (2017).